Weak localization of polaritons and the generation of phase-conjugated light waves

Eiichi Hanamura
Department of Applied Physics, University of Tokyo, Hongo, Bunkyo-ku, Tokyo 113, Japan
(Received 21 June 1988)

The microscopic mechanism of generation of phase-conjugated light waves is presented in terms of weak localization of polaritons. Phase-conjugated waves, which are the time-reversal propagation of probe light, are shown to be enhanced by constructive interference between elastic multiple scattering of polaritons at impurities and time-reversed processes. This is characteristic of the time-reversal invariance of the system. We list several characteristics of generation of phase-conjugated waves due to the weak localization of polaritons. These observations will be applied to check the present theory.

I. INTRODUCTION

The propagation of a wave in a dense distribution of elastic scatterers shows many interesting phenomena. For example, constructive interferences arise for the backscattering in the direction opposite to the incident one, and this explains the enhancement of the backscattered intensity with respect to the classical prediction. This phenomenon has been recognized almost independently in two different fields. In condensed-matter physics, it is the basis of the weak-localization regime for electrons in impure metals, which led to dimensional dependence of Anderson localization.[1,2] In optics, since the pioneering work by de Wolf,[3] the intensity of light scattering from disordered media has been observed to show a sharp peak centered at the backscattering direction as well as the polarization dependence of the scattered light.[4–9] Weak localization of phonons was also discussed.[10]

The basis of the interference effect in multiple scattering is very general. Consider a sequence of n scattering events characterized by the wave vectors $\mathbf{k}_i, \mathbf{k}_1, \mathbf{k}_2, \ldots, \mathbf{k}_n = \mathbf{k}_f$, where $\mathbf{k}_j$ is the wave vector after the jth scattering event and $\mathbf{k}_i$ and $\mathbf{k}_f$ stand for the initial and final wave vectors. In classical transport theory, all n-order sequences are assumed to be uncorrelated as result of the random nature of the distribution of scatterers. However, any given sequence and its time reverse $\mathbf{k}_i, -\mathbf{k}_{n-1}, -\mathbf{k}_{n-2}, \ldots, -\mathbf{k}_1, \mathbf{k}_f$, where the light is scattered by the same centers but in opposite order, can interfere constructively for a special choice of $\mathbf{k}_f$ relative to $\mathbf{k}_i$.[11] This coherent superposition comes from the time invariance of the present system.

On the other hand, phase conjunction is defined as the process in which the phase of the output wave is a complex conjugate to the phase of an input wave. If the phase-conjugated output propagates in the backward direction with respect to the corresponding input wave, then it can be used to correct aberration due to the phase distortion experienced by the input wave.[12] This is also one of the degenerate four-wave mixings and can be understood from the following physical picture. Under three input waves with a common frequency ω_0, i.e., forward ($\mathbf{k}_0$) and backward ($-\mathbf{k}_0$) pump waves and probe wave ($\mathbf{k}_i$), the signal wave ($\mathbf{k}_s$) is possible in three directions $\mathbf{k}_s = \mathbf{k}_i \pm 2\mathbf{k}_0$ and $\mathbf{k}_s = -\mathbf{k}_i$. However, as $|\mathbf{k}_s|$ is not, in general, equal to $\omega_0(\epsilon_\infty)^{1/2}/c$, the generation in the directions $\mathbf{k}_i \pm 2\mathbf{k}_0$ may not be phase matched but that in $\mathbf{k}_s = -\mathbf{k}_i$ is always phase matched. Here ϵ_∞ is an optical dielectric constant. This is the phase-conjugated wave of the probe wave $\mathbf{k}_i$.

Here arises a question to microscopic understanding of generation of the phase-conjugated wave. We will point out in this paper that the weak localization of excitons or polaritons plays key roles in generation of the phase-conjugated wave for the cases of using excitons or polaritons as the nonlinear optical medium. The phase-conjugated wave is the time-reversal propagation of the probe light. We will microscopically describe formation of the population grating from one of the pump waves and the probe wave and reflection of the other pump wave by the grating in terms of multiple elastic scatterings of polaritons at impurities. This will be shown to be related with elementary excitations which are precursors of the Anderson localization and are also characteristic of the time-reversal invariance of the material system. These elementary excitations in metals have been called "cooperons" and "diffusions."[13]

In Sec. II, we introduce a model of four-wave mixing under nearly resonant pumping of excitons, and derive the Hamiltonian of polaritons in the crystal with elastic scatterers under external pump fields. In Sec. III, we formulate the third-order optical processes in which a signal polariton is produced in terms of Green's functions of polaritons. Then we will show in Sec. IV that the vertex part describing coherent superposition of the forward- and backward-propagating waves induced by multiple elastic scatterings at impurities, plays the important roles in formation of the population gratings and reflection of the third wave by the grating. This vertex part has singularities in the difference of two input frequencies and in the sum or difference of two wave vectors of relevant polaritons. We will discuss in Sec. V the conventional case in which multiple elastic scatterings do not play any roles. The generation of the phase-conjugated wave is quantitatively discussed referring to the case of exciton

polaritons in CuCl in Sec. VI and Sec. VII in terms of the results in the preceding two sections. Section VII is devoted to discussion and conclusion. Particularly, several characteristics of the phase-conjugated wave due to the weak localization of exciton polaritons are demonstrated. These observations will work as confirmation of the present theory.

II. POLARITONS IN THE CRYSTAL WITH IMPURITIES

We consider a crystal much larger than a relevant optical wavelength $\lambda=2\pi c/(\epsilon_\infty)^{1/2}\omega_0$ in the medium. Here c is a light velocity in vacuum, ϵ_∞ is an optical dielectric constant, and ω_0 is an angular frequency of an exciton. An exciton $(b_{\nu\mathbf{k}},b^\dagger_{\nu\mathbf{k}})$ in a quantum state ν for the electron-hole relative motion and a wave-number vector $\mathbf{k}$ for the center-of-mass motion, interacts with a radiation field $(a_{\alpha\mathbf{k}},a^\dagger_{\alpha\mathbf{k}})$ with a polarization α and the same wave-number vector $\mathbf{k}$ as the exciton inside the crystal. The Hamiltonian of this system is written in the following form:

$$H_0=\sum_{\nu\mathbf{k}}\{\hbar c^* k a^\dagger_{\alpha\mathbf{k}}a_{\alpha\mathbf{k}}+E_\nu(\mathbf{k})b^\dagger_{\nu\mathbf{k}}b_{\nu\mathbf{k}} -iA_{\mathbf{k}}[(a_{\alpha\mathbf{k}}+a^\dagger_{\alpha-\mathbf{k}})b^\dagger_{\nu\mathbf{k}}-(a_{\alpha-\mathbf{k}}+a^\dagger_{\alpha\mathbf{k}})b_{\nu\mathbf{k}}]\}\ , \tag{1}$$

where $c^*=c/(\epsilon_\infty)^{1/2}$ is light velocity in the crystal and $E_\nu(\mathbf{k})$ is energy of an exciton in the quantum state $(\nu,\mathbf{k})$. A coupling constant $A_{\mathbf{k}}$ of an exciton and a photon with the same polarization as the exciton is written as follows:

$$A_{\mathbf{k}}=\left[\frac{2\pi}{\hbar c^* k}\right]^{1/2}E_\nu(\mathbf{k})\Phi_\nu(0)\mu_{cv}\ , \tag{2}$$

with $\Phi_{1s}(0)=(\pi a_B^3)^{-1/2}$. Here, $\Phi_\nu(0)$ is a wave function of the electron-hole relative motion at origin in the eigenstate ν, a_B an exciton Bohr radius in the lowest eigenstate $\nu=1s$ for the relative motion, and μ_{cv} the transition dipole moment between the relevant valence and conduction bands. The exciton-photon coupling constant $A_{\mathbf{k}}$ is much larger than other interactions in many cases, to which we will confine ourselves in the present paper. Therefore, we diagonalize first the Hamiltonian (1) in terms of the hybridized modes of polaritons under the transformation[14]

$$(c_{\mathbf{k}1},c_{\mathbf{k}2},c^\dagger_{-\mathbf{k}1},c^\dagger_{-\mathbf{k}2})=C(a_{\alpha\mathbf{k}},b_{\nu\mathbf{k}},a^\dagger_{\alpha-\mathbf{k}},b^\dagger_{\nu-\mathbf{k}})\ . \tag{3}$$

Then we have the polariton Hamiltonian

$$H_0=\sum_{\mathbf{k}\alpha}\hbar\omega_\alpha(\mathbf{k})c^\dagger_{\mathbf{k}\alpha}c_{\mathbf{k}\alpha}\ , \tag{4}$$

where $c_{\mathbf{k}\alpha}$ and $c^\dagger_{\mathbf{k}\alpha}$ are annihilation and creation operators of polaritons with the wave-number vector $\mathbf{k}$ and α denotes both the branch (upper or lower) and the polarization direction. The eigenfrequencies $\omega_\alpha(\mathbf{k})$ of polaritons are obtained as solutions of the following dispersion relation:[14]

$$\epsilon\equiv\left[\frac{c^*k}{\omega}\right]^2=1+\frac{4\pi\beta}{1-[\hbar\omega/E_0(\mathbf{k})]^2}\ ,$$

with

$$\beta\equiv 2E_0(\mathbf{k})\frac{|\mu_{cv}|^2}{\pi\hbar^2a_B^3}=\frac{e^2}{m}f_{1s}\ .$$

Here $E_0(\mathbf{k})$ denotes an exciton dispersion in the lowest state $\nu=1s$, and f_{1s} is an oscillator strength for the state $\nu=1s$. We are interested in excitation around the lowest exciton state with the largest oscillator strength, especially in its lower branch of polaritons. Therefore, we will skip the suffix α specifying the branch and the polarization of polaritons and we will use a unit $\hbar=1$ hereafter.

The exciton is scattered elastically by the impurity potential $\sum_i V(\mathbf{r}-\mathbf{r}_i)$:

$$V=\int d\mathbf{r}\,\phi^\dagger_{\rm exc}(\mathbf{r})\sum_i V(\mathbf{r}-\mathbf{r}_i)\phi_{\rm exc}(\mathbf{r}) =\sum_{i\mu\nu\mathbf{kq}}V_{\mu\nu}(\mathbf{q})\exp(i\mathbf{q}\cdot\mathbf{r}_i)b^\dagger_{\nu\mathbf{k}+\mathbf{q}}b_{\mu\mathbf{k}}\ . \tag{5}$$

This scattering Hamiltonian is rewritten in terms of the polariton operators $(c_{\mathbf{k}\alpha},c^\dagger_{\mathbf{k}\alpha})$ using Eq. (3) and we keep only the elastic scattering on the polariton dispersion in the lower branch. Then V of Eq. (5) is simplified into the following form:

$$V=\sum_{\mathbf{k},\mathbf{q}}V(\mathbf{q})c^\dagger_{\mathbf{k}+\mathbf{q}}c_{\mathbf{k}}\ ,$$

where $V(\mathbf{q})\equiv\sum_i V_0(\mathbf{q})\exp(i\mathbf{q}\cdot\mathbf{r}_i)$ and is described by $V_{\mu\nu}(\mathbf{q})$ in Eq. (5) and transformation matrix elements C in Eq. (3). As a result, the material system is described by the Hamiltonian

$$H=H_0+V=\sum_{\mathbf{k}}\omega(\mathbf{k})c^\dagger_{\mathbf{k}}c_{\mathbf{k}}+\sum_{\mathbf{kq},i}V_0(\mathbf{q})\exp(i\mathbf{q}\cdot\mathbf{r}_i)c^\dagger_{\mathbf{k}+\mathbf{q}}c_{\mathbf{k}}\ . \tag{6}$$

Next we have to consider the effect of external radiation fields on the material system. The ground state of a material system $|0\rangle$ is a vacuum of any kind of polaritons. The radiation field was considered to be divided into those in two spaces inside and outside the crystal. The former was taken into account already in forming the polaritons. The external radiation fields $\mathbf{E}_{\rm ext}$ excite the polaritons at the crystal surface. This process is described by the interaction Hamiltonian H':

$$H'=\sum_{\alpha,j,\mathbf{k}}(c_{\mathbf{k}\alpha}+c^\dagger_{\mathbf{k}\alpha})\boldsymbol{\mu}_\alpha\cdot\mathbf{E}_j\ , \tag{7}$$

where $\boldsymbol{\mu}_\alpha$ is the polarization vector of the polariton (α) and is evaluated in terms of the exciton dipole moment and the transformation matrix elements C. External field $\mathbf{E}_j$ with an angular frequency ω_j can excite the polariton with the same frequency $\omega(\mathbf{k})=\omega_j$ with the wave-number vector $\mathbf{k}$ which is determined by the incident angle and the polariton dispersion. The wave-number vector $\mathbf{k}$ and $\boldsymbol{\mu}_\alpha$ can also be determined classically in terms of the reflection constant (or refractive index) and the incident frequency. The signal polaritons are produced through nonlinear processes which will be discussed in the following sections. These polaritons can be taken out to outside the crystal as signal lights. This process is described also

by Eq. (7) and can also be classically determined in terms of the refractive index and the angle hitting the surface from inside the crystal. Therefore, we will pursue the generation of phase-conjugated polariton waves through the excitations of the time-invariant collective modes in impure crystals in the following sections.

III. THIRD-ORDER NONLINEAR OPTICAL PROCESSES

The amplitude of the phase-conjugated wave is derived by two steps. First, we derive third-order perturbations of the density matrix in the polariton-external field interaction H' and obtain the expression for an amplitude of signal polariton through four-wave mixing. Second, in terms of this expression, we take into account effects of elastic multiple scatterings of polaritons at impurities. Then we will be able to give microscopic expressions for formation of population gratings due to two input polaritons and reflection of the third input polariton by the gratings. In this section, we will specify the expression for the amplitude of the phase-conjugated wave among processes of the general four-wave mixings.

The amplitude of signal polariton is expressed as[15,16]

$$\langle c_{\mathbf{K}_s}(\omega_s)\rangle \equiv \int_{-\infty}^{\infty} dt\, e^{i\omega_s t}\langle\langle c_{\mathbf{K}_s}|\rho(t)\rangle\rangle = \int_{-\infty}^{\infty} dt\, e^{i\omega_s t}\langle \mathrm{Tr} c_{\mathbf{K}_s}\rho(t)\rangle ,$$

where $\rho(t)$ is a density matrix of the total system $H_T=H+H'$, and the double angular brackets mean taking the ensemble average over the impurity distribution as well as the quantum-mechanical average. A state $\langle c_{\mathbf{K}_s}|$ is a Hermitian conjugate of a single-polariton state $c^{\dagger}_{\mathbf{K}_s}|0\rangle$. The density matrix $\rho(t)=\exp(-iH_T t)\rho_0\exp(iH_T t)$ is expanded to the third order of H', where ρ_0 denotes the crystal ground state $|0\rangle\langle 0|$. Then we have a familiar expression[17,18]

$$\langle c_{\mathbf{K}_s}(\omega_s)\rangle = (-i)^3\int_{-\infty}^{\infty} dt\, e^{i\omega_s t}\int_{-\infty}^{t} dt_3\int_{-\infty}^{t_3} dt_2\int_{-\infty}^{t_2} dt_1\langle\langle c_{\mathbf{K}_s}[H'(t_3),[H'(t_2),[H'(t_1),\rho_0]]]\rangle\rangle . \quad (8)$$

The result is independent of the value of the lower bounds in the three integrals, as will be shown later. Here we take $-\infty$ as in Refs. 17 and 18. Here we apply three input optical fields as external field $\mathbf{E}_{\mathrm{ext}}$: (1) forward pump field $(\omega_0,\mathbf{K}_0)$, (2) backward pump field $(\omega_0,-\mathbf{K}_0)$, and (3) probe field $(\omega_i,\mathbf{K}_i)$. Here, and hereafter, we consider a case under nearly resonant pumping of the lowest exciton so that a rotating-wave approximation is well justified. Three commutators in Eq. (8) bring about eight terms, but only four kinds of diagrams drawn in Fig. 1 contribute to the four-wave mixing under a rotating-wave approximation. In the diagrams in Fig. 1, we have denoted $(\omega_1,\mathbf{K}_1)$, $(\omega_2,\mathbf{K}_2)$, and $(\omega_3,\mathbf{K}_3)$ as polaritons generated by input fields at times t_1 (or t_2), t_2 (or t_1), and t_3, respectively. There are six combinations of these three input fields for each diagram in Fig. 1 so that we have a total of 24 contributions, as shown in Table I. Then we get three kinds of signal polaritons $(\omega_s=\omega_i,\ \mathbf{K}_s=\mathbf{K}_i\pm 2\mathbf{K}_0)$ and $(\omega_s=2\omega_0-\omega_i,\ \mathbf{K}_s=-\mathbf{K}_i)$. The last wave corresponds to generation of a polariton wave phase conjugated to the probe field $(\omega_i,\mathbf{K}_i)$ for the degenerate case $\omega_0=\omega_i=\omega_s$. As shown in Table I, the phase-conjugated

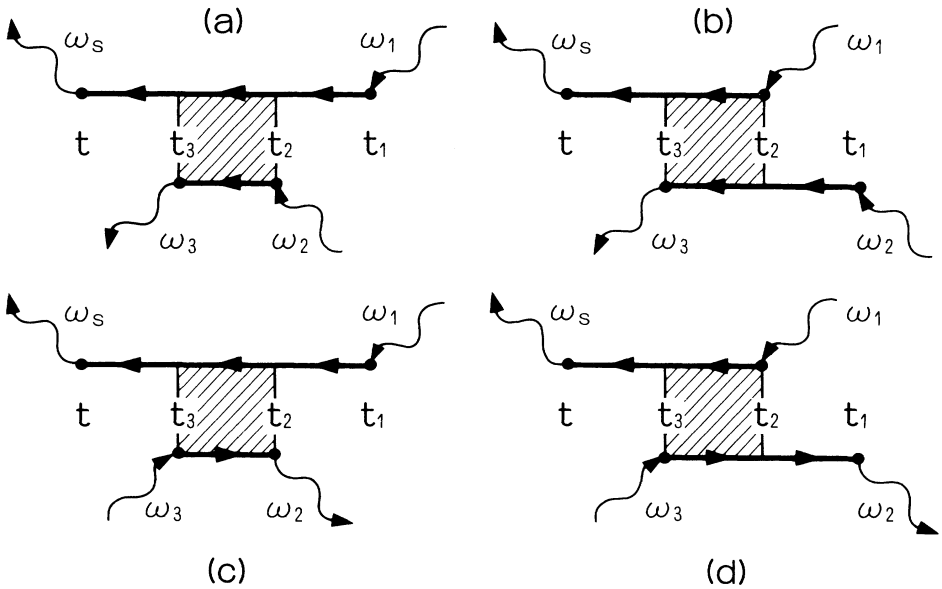

FIG. 1. Feynman diagrams describing four kinds of contributions to four-wave mixing under the rotating-wave approximation. The leftward and rightward arrows denote the corresponding propagations of states in the density matrix. Time development in the diagram is leftward. ω_1, ω_2, and ω_3 represent three input fields and ω_s represents the signal at time t.

TABLE I. Twenty-four cases contributing to four-wave mixing of ω_1, ω_2, and ω_3 input waves. The cases a, b, c, and d correspond, respectively, to the processes of the Feynman diagrams in Figs. 1(a), 1(b), 1(c), and 1(d), with the described combinations of forward- and backward-pump waves and probe waves. ω_s and $\mathbf{K}_s$ denote, respectively, the signal angular frequency and signal wave-number vector. $\mathbf{E}_s$ describes the polarization dependence of the signal wave on the polarizations of three input waves.

Case		ω_1	ω_2	ω_3	ω_s	$\mathbf{E}_s$
I	a	$\omega_0\mp\mathbf{K}_0$	$\omega_i\mathbf{K}_i$	$\omega_0\pm\mathbf{K}_0$	$\omega_s=\omega_i$	$(\mathbf{E}_i\cdot\mathbf{E}_\mp)\mathbf{E}_\pm$
	b				$\mathbf{K}_s=\mathbf{K}_i\mp2\mathbf{K}_0$	
	c				$\omega_s=2\omega_0-\omega_1$	
	d				$\mathbf{K}_s=-\mathbf{K}_i$.	
II	a	$\omega_i\mathbf{K}_i$	$\omega_0\mp\mathbf{K}_0$	$\omega_0\pm\mathbf{K}_0$	$\omega_s=\omega_i$	$(\mathbf{E}_i\cdot\mathbf{E}_\mp)\mathbf{E}_\pm$
	b				$\mathbf{K}_s=\mathbf{K}_i\mp2\mathbf{K}_0$	
	c				$\omega_s=\omega_i$	
	d				$\mathbf{K}_s=\mathbf{K}_i\pm2\mathbf{K}_0$	
III	a	$\omega_0\mp\mathbf{K}_0$	$\omega_0\pm\mathbf{K}_0$	$\omega_i\mathbf{K}_i$	$\omega_s=2\omega_0-\omega_i$	$(\mathbf{E}_\mp\cdot\mathbf{E}_\pm)\mathbf{E}_i$
	b				$\mathbf{K}_s=-\mathbf{K}_i$	
	c				$\omega_s=\omega_i$	
	d				$\mathbf{K}_s=\mathbf{K}_i\mp2\mathbf{K}_0$	

wave is generated in cases Ic and Id, i.e., diagrams (c) and (d) of Fig. 1 with $\omega_1=(\omega_0,\mp\mathbf{K}_0)$, $\omega_2=(\omega_i,\mathbf{K}_1)$, and $\omega_3=(\omega_0,\pm\mathbf{K}_0)$, and in cases IIIa and IIIb, i.e., diagrams (a) and (b) of Fig. 1 with $\omega_1=(\omega_0,\mp\mathbf{K}_0)$, $\omega_2=(\omega_0,\pm\mathbf{K}_0)$, and $\omega_3=(\omega_i,\mathbf{K}_i)$. We will show evaluation of $\langle c_{\mathbf{K}_s}(\omega_s)\rangle$ for case Ic as an example:

$$\langle\langle c_{\mathbf{K}_s}(t)H'(\mathbf{K}_0,t_3)\rho_0H'(\mathbf{K}_i,t_2)H'(-\mathbf{K}_0,t_1)\rangle\rangle = A\langle G(t,t_3,t_2,t_1)\rangle\ , \tag{9}$$

where

$$A=\langle 0|c_{\mathbf{K}_s}|\omega_s\mathbf{K}_s\rangle\langle\omega_0\mathbf{K}_0|c^\dagger_{\mathbf{K}_0}\boldsymbol{\mu}\cdot\mathbf{E}(\mathbf{K}_0)|0\rangle \times\langle 0|c_{\mathbf{K}_i}\boldsymbol{\mu}\cdot\mathbf{E}(\mathbf{K}_i)^*|\omega_i\mathbf{K}_i\rangle \times\langle\omega_0-\mathbf{K}_0|c^\dagger_{-\mathbf{K}_0}\boldsymbol{\mu}\cdot\mathbf{E}(-\mathbf{K}_0)|0\rangle\ , \tag{9a}$$

and

$$G(t,t_3,t_2,t_1) =(-i)^3\langle\omega_s\mathbf{K}_s|e^{-H(t-t_1)}|\omega_0\mathbf{K}_0\rangle e^{-i\omega_0t_1} \times e^{i\omega_it_2}\langle\omega_i\mathbf{K}_i|e^{iH(t_2-t_3)}|\omega_0-\mathbf{K}_0\rangle e^{-i\omega_0t_3}\ . \tag{9b}$$

Here the time interval (t,t_1) is divided into three parts (t,t_3), (t_3,t_2), and (t_2,t_1) as shown in Fig. 1. Then an ensemble average of G over the impurity distribution for the time interval (t,t_1) is approximated by a product of three ensemble averages for (t,t_3), (t_3,t_2), and (t_2,t_1) as follows:

$$\langle G(t,t_3,t_2,t_1)\rangle=(-i)^3e^{-i(2\omega_0-\omega_i)t}e^{i\omega_s(t-t_3)}\langle\langle\omega_s\mathbf{K}_s|e^{-iH(t-t_3)}|\omega_s'\mathbf{K}_s'\rangle_+\rangle \times e^{i(\omega_0-\omega_i)(t_3-t_2)}\langle\langle\omega_s'\mathbf{K}_s'|e^{-iH(t_3-t_2)}|\omega_0'\mathbf{K}_0'\rangle_+\langle\omega_i\mathbf{K}_i|e^{iH(t_3-t_2)}|\omega_0-\mathbf{K}_0\rangle_-\rangle \times e^{i\omega_0(t_2-t_1)}\langle\langle\omega_0'\mathbf{K}_0'|e^{-iH(t_2-t_1)}|\omega_0\mathbf{K}_0\rangle_+\rangle\ .$$

Then a contribution of case Ic in Table I to $\langle c_{\mathbf{K}_s}(\omega_s)\rangle$ is expressed in terms of three propagators as follows:

$$\langle c_{\mathbf{K}_s}(\omega_s)\rangle_c=A\int_{-\infty}^{\infty}dt\,e^{i(\omega_s-2\omega_0+\omega_i)t}\int_{-\infty}^{t}dt_3\int_{-\infty}^{t_3}dt_2\int_{-\infty}^{t_2}dt_1G_s(t-t_3)\Xi(t_3-t_2)G_f(t_2-t_1) =A\int_{-\infty}^{\infty}dt\,e^{i(\omega_s-2\omega_0+\omega_i)t}\int_0^{\infty}G_s(\tau_3)d\tau_3\int_0^{\infty}\Xi(\tau_2)d\tau_2\int_0^{\infty}G_f(\tau_1)d\tau_1\ . \tag{10}$$

Here

$$G_s(\tau_3)=-ie^{i\omega_s\tau_3}\langle\langle\omega_s\mathbf{K}_s|e^{-iH\tau_3}|\omega_s'\mathbf{K}_s'\rangle_+\rangle\ , \tag{11a}$$

$$\Xi(\tau_2)=-ie^{i(\omega_0-\omega_i)\tau_2}\langle\langle\omega_s'\mathbf{K}_s'|e^{-iH\tau_2}|\omega_0\mathbf{K}_0\rangle_+ \times\langle\omega_i\mathbf{K}_i|e^{iH\tau_2}|\omega_0-\mathbf{K}_0\rangle_-\rangle\ , \tag{11b}$$

$$G_f(\tau_1)=-ie^{i\omega_0\tau_1}\langle\langle\omega_0'\mathbf{K}_0'|e^{-iH\tau_1}|\omega_0\mathbf{K}_0\rangle_+\rangle\ . \tag{11c}$$

Here we used abbreviation $|\omega_s'\mathbf{K}_s'\rangle\langle\omega_s'\mathbf{K}_s'| =\sum_{\omega_s'\mathbf{K}_s'}|\omega_s'\mathbf{K}_s'\rangle\langle\omega_s'\mathbf{K}_s'|$, which is equal to 1. Propagators $G(t)$ describe propagation of polaritons $(\omega_0,\mathbf{K}_0)$ and $(\omega_s,\mathbf{K}_s)$ in a crystal with elastic scatterers. It is the vertex part Ξ that represents formation of population gratings of polaritons as well as generation of the conjugated

wave $(\omega_s,\mathbf{K}_s)$ due to reflection of one of the pump fields by the population grating. Suffixes + and − of the inner brackets in Eq. (11) mean the leftward and rightward propagations of the states in the density matrix as also realized in Fig. 1(c).

Contribution of the diagram of Fig. 1(d) is obtained by replacing the last propagator $G_f(\tau_1)$ in Eq. (10) by

$$G_b(\tau)=-ie^{-i\omega_0\tau}\langle\langle\omega_0'-\mathbf{K}_0'|e^{-iH\tau}|\omega_0-\mathbf{K}_0\rangle_-\rangle\ .$$

Contributions to $\langle\langle c_{\mathbf{K}_s}(\omega_s)\rangle\rangle$ from cases Ic and Id in Table I with $\mathbf{K}_0$ and $-\mathbf{K}_0$ exchanged are obtained from the above results by exchanging $\mathbf{K}_0$ and $-\mathbf{K}_0$. These give the same results besides the factor A given by Eq. (9a) as long as $\omega(-\mathbf{K}_0)=\omega(\mathbf{K}_0)$.

IV. MICROSCOPIC DESCRIPTION OF GRATING FORMATION

Effects of elastic scatterings of polaritons by impurity centers are evaluated in this section. Only a single polariton propagates for time intervals (t_2,t_1) and (t,t_3) in all diagrams in Fig. 1. For the diagram of Fig. 1(c) with a combination case Ic in Table I, which we discussed in Sec. III, the forward pump polariton $(\omega_0,\mathbf{K}_0)$ propagates for the initial interval (t_2,t_1) while the signal polariton does so in the last interval (t,t_3). For the intermediate interval (t_3,t_2), polaritons $(\omega_0,\mathbf{K}_0)$, and $(\omega_i,\mathbf{K}_i)$ propagating, respectively, in the leftward and rightward directions in the density matrix form the population grating with the difference wave-number vector $\mathbf{K}_0-\mathbf{K}_i$ and oscillating in time with the difference frequency $\omega_0-\omega_i$. Then the third polariton $(\omega_0,-\mathbf{K}_0)$ is reflected by this grating and the phase-conjugated wave $(\omega_s=2\omega_0-\omega_i,\ \mathbf{K}_s=-\mathbf{K}_i)$ is generated as a signal polariton. Therefore the vertex part plays the key role in generation of the phase-conjugated wave.

Integrals in time in Eq. (10) are performed using perturbational expansions of the propagators in the polariton-scatterers interaction V of Eq. (6)

$$e^{-iHt}=e^{-iH_0t}-i\int_0^t dt_1 e^{-iH_0(t-t_1)}Ve^{-iH_0t_1}+(-i)^2\int_0^t dt_1\int_0^{t_1}dt_2 e^{-iH_0(t-t_1)}Ve^{-iH_0(t_1-t_2)}Ve^{-iH_0t_2}\cdots\ , \tag{12a}$$

$$e^{iHt}=e^{iH_0t}+i\int_0^t dt_1 e^{iH_0(t-t_1)}Ve^{iH_0t_1}+i^2\int_0^t dt_1\int_0^{t_1}dt_2 e^{iH_0t_2}Ve^{iH_0(t_1-t_2)}Ve^{iH_0(t-t_1)}\cdots\ . \tag{12b}$$

Equations (11a) and (11c) represent a single polariton propagation which is described by a retarded Green's function

$$\begin{aligned}&G^R(\omega_0,\mathbf{K}_0)\\&=-i\int_0^\infty d\tau e^{i\omega_0\tau}\langle\langle\omega_0'\mathbf{K}_0'|e^{-iH\tau}|\omega_0\mathbf{K}_0\rangle_+\rangle\\&=\frac{1}{\omega_0-\omega(\mathbf{K}_0)-\Sigma(\mathbf{K}_0,\omega_0)}\delta_{\omega_0\omega_0'}\delta_{\mathbf{K}_0\mathbf{K}_0'}\ ,\end{aligned} \tag{13a}$$

$$\begin{aligned}&G^R(\omega_s,\mathbf{K}_s)\\&=-i\int_0^\infty d\tau e^{i\omega_s\tau}\langle\langle\omega_s\mathbf{K}_s|e^{-iH\tau}|\omega_s'\mathbf{K}_s'\rangle_+\rangle\\&=\frac{1}{\omega_s-\omega(\mathbf{K}_s)-\Sigma(\mathbf{K}_s,\omega_s)}\delta_{\omega_s\omega_s'}\delta_{\mathbf{K}_s\mathbf{K}_s'}\ ,\end{aligned} \tag{13b}$$

where the self-energy $\Sigma(\mathbf{K},\omega)$ is evaluated to the lowest order in the concentration n_i of the elastic scattering centers as shown by the diagram of Fig. 2(a). A Fourier

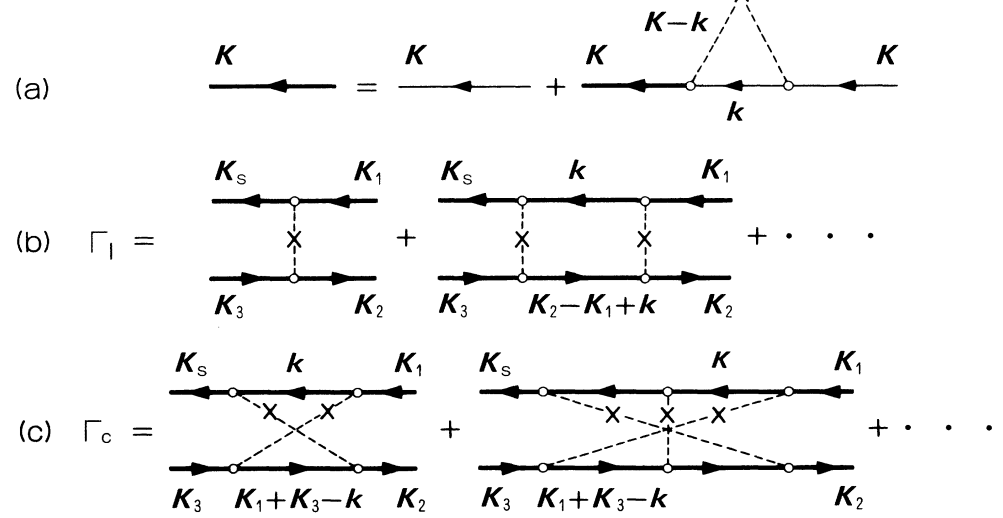

FIG. 2. (a) Diagram describing the lowest-order contribution to the self-energy of polariton $\mathbf{K}$. The cross and dotted lines mean a scattering center and elastic scatterings of polariton. (b) Ladderlike scatterings of the leftward and rightward polaritons. (c) The maximally crossed scattering mechanism of polaritons at impurity centers.

transform of a scattering potential at a single site $\mathbf{R}_i$ is expressed as

$$\frac{1}{\Omega}\int V(\mathbf{r}-\mathbf{R}_i)e^{i(\mathbf{K}-\mathbf{K}')\cdot\mathbf{r}}d\mathbf{r}=V_0(\mathbf{K}-\mathbf{K}')e^{i(\mathbf{K}-\mathbf{K}')\cdot\mathbf{R}_i}\ , \tag{14}$$

where Ω is a volume of the crystal. The second-order scattering shown in Fig. 2(a) gives the lowest-order contribution as realized by taking the ensemble average of products of impurity scattering potentials Eq. (14) over uniform distribution of scatterers. Then the result is

$$\begin{aligned}\Sigma(\mathbf{K},\omega)&=-i\pi N(\omega)n_i\int\frac{d\Omega}{4\pi}|V_0(\mathbf{K}-\mathbf{K}')|^2\\&\doteqdot -i\pi N(\omega)n_i|V(0)|^2\\&\equiv -i\gamma\ .\end{aligned}\tag{15}$$

Here $N(\omega)$ is the state density of the polariton and the integral means an angle average over a sphere. The polariton is electrically neutral and has long wavelength so that impurity potential $V(\mathbf{r}-\mathbf{R}_i)$ is considered to be of a short-range and wave-vector dependence of $V_0(\mathbf{K}-\mathbf{K}')$ which was neglected in Eq. (15). This constant is abbreviated as $V(0)$ here and hereafter.

A vertex part Ξ of Eq. (11b) describes formation of population grating of polaritons and generation of phase-conjugated wave for the time interval (t_2,t_3). Coherent effects in the elastic multiple scatterings of polaritons are taken into account. It is shown that constructive interference between time-reversed paths of the polariton results in enhanced generation of the phase-conjugated wave. The vertex part is calculated in two steps in the following. First, perturbation expansions of Eqs. (12a) and (12b) are inserted in the expression of Ξ in Eq. (11b):

$$\Xi(\omega_0-\omega_i)\equiv\int_0^\infty\Xi(\tau_2)d\tau_2$$

$$=-i\int_0^\infty dt\,e^{i(\omega_0-\omega_i)t}\langle\langle\omega_s\mathbf{K}_s|e^{-iHt}|\omega_0\mathbf{K}_0\rangle_+\langle\omega_i\mathbf{K}_i|e^{iHt}|\omega_0'-\mathbf{K}_0'\rangle_-\rangle \tag{16a}$$

$$\begin{aligned}&=-i\sum_{n=0}^\infty\sum_{m=0}^\infty\int_0^\infty dt\,e^{i[\omega_0-\omega_i-\omega(\mathbf{K}_0)+\omega(\mathbf{K}_i)]t}(-i)^n i^m\\&\times\int_0^t dt_1\int_0^{t_1}dt_2\cdots\int_0^{t_{n-1}}dt_n\int_0^t dt_1'\int_0^{t_1'}dt_2'\cdots\int_0^{t_{m-1}'}dt_m'\sum_{\mathbf{q}_i}\cdots\sum_{\mathbf{q}_{n-1}}\sum_{\mathbf{q}_1'}\cdots\sum_{\mathbf{q}_{m-1}'}\\&\times\langle e^{-i[\omega(\mathbf{K}_s)-\omega(\mathbf{K}_0)](t-t_1)}V_{\mathbf{K}_s\mathbf{q}_1}e^{-i[\omega(\mathbf{q}_1)-\omega(\mathbf{K}_0)](t_1-t_2)}V_{\mathbf{q}_1\mathbf{q}_2}\cdots e^{-i[\omega(\mathbf{q}_{n-1})-\omega(\mathbf{K}_0)](t_{n-1}-t_n)}V_{\mathbf{q}_{n-1}\mathbf{K}_0}V_{\mathbf{K}_i\mathbf{q}_{m-1}'}\\&\quad\times e^{i[\omega(\mathbf{q}_{m-1}')-\omega(\mathbf{K}_i)](t_{m-1}'-t_m')}V_{\mathbf{q}_{m-1}'\mathbf{q}_{m-2}'}\cdots V_{\mathbf{q}_1'-\mathbf{K}_0'}e^{i[\omega(-\mathbf{K}_0')-\omega(\mathbf{K}_i)](t-t_1')}\rangle\end{aligned} \tag{16b}$$

$$\begin{aligned}&=-i\sum_{n=0}^\infty\sum_{m=0}^\infty\int_0^\infty dt\,e^{i[\omega_0-\omega_i-\omega(\mathbf{K}_0)+\omega(\mathbf{K}_i)+2i\gamma_0]t}\sum_{\mathbf{q}_1}\cdots\sum_{\mathbf{q}_{n-1}}\sum_{\mathbf{q}_1'}\cdots\sum_{\mathbf{q}_{m-1}'}\\&\times(-i)^n i^m\int_0^\infty d\tau_1\int_0^\infty d\tau_2\cdots\int_0^\infty d\tau_n\int_0^\infty d\tau_1'\int_0^\infty d\tau_2'\cdots\int_0^\infty d\tau_m'\\&\times\langle e^{-i[\omega(\mathbf{K}_s)-\omega(\mathbf{K}_0)-i\gamma_0]\tau_1}V_{\mathbf{K}_s\mathbf{q}_1}e^{-i[\omega(\mathbf{q}_1)-\omega(\mathbf{K}_0)-i\gamma_0]\tau_2}V_{\mathbf{q}_1\mathbf{q}_2}e^{-i[\omega(\mathbf{q}_2)-\omega(\mathbf{K}_0)-i\gamma_0]\tau_3}\cdots\\&\quad\times e^{-i[\omega(\mathbf{q}_{n-1})-\omega(\mathbf{K}_0)-i\gamma_0]\tau_n}V_{\mathbf{q}_{n-1}\mathbf{K}_0}V_{\mathbf{K}_i\mathbf{q}_{m-1}'}\\&\quad\times e^{i[\omega(\mathbf{q}_{m-1}')-\omega(\mathbf{K}_i)+i\gamma_0]\tau_m'}V_{\mathbf{q}_{m-1}'\mathbf{q}_{m-2}'}e^{i[\omega(\mathbf{q}_{m-2}')-\omega(\mathbf{K}_i)+i\gamma_0]\tau_{m-1}'}\cdots\\&\quad\times e^{i[\omega(\mathbf{q}_1')-\omega(\mathbf{K}_i)+i\gamma_0]\tau_1'}V_{\mathbf{q}_1'-\mathbf{K}_0'}e^{i[\omega(-\mathbf{K}_0')-\omega(\mathbf{K}_i)+i\gamma_0]\tau_1'}\rangle\end{aligned} \tag{16c}$$

$$\begin{aligned}&=\frac{-i}{2\gamma_0}\sum_{n=0}^\infty\sum_{m=0}^\infty\sum_{\mathbf{q}_1}\cdots\sum_{\mathbf{q}_{n-1}}\sum_{\mathbf{q}_1'}\cdots\sum_{\mathbf{q}_{m-1}'}\delta_{\mathbf{K}_0-\mathbf{K}_s,\mathbf{K}_0'+\mathbf{K}_i}\\&\times\left\langle\frac{1}{\omega(\mathbf{K}_0)-\omega(\mathbf{K}_s)+i\gamma_0}V_{\mathbf{K}_s\mathbf{q}_1}\frac{1}{\omega(\mathbf{K}_0)-\omega(\mathbf{q}_1)+i\gamma_0}V_{\mathbf{q}_1\mathbf{q}_2}\cdots\right.\\&\quad\times\frac{1}{\omega(\mathbf{K}_0)-\omega(\mathbf{q}_{n-1})+i\gamma_0}V_{\mathbf{q}_{n-1}\mathbf{K}_0}V_{\mathbf{K}_i\mathbf{q}_{m-1}'}\frac{1}{\omega(\mathbf{K}_i)-\omega(\mathbf{q}_{m-1}')-i\gamma_0}\\&\quad\times V_{\mathbf{q}_{m-1}'\mathbf{q}_{m-2}'}\cdots\frac{1}{\omega(\mathbf{K}_i)-\omega(\mathbf{q}_1')-i\gamma_0}V_{\mathbf{q}_1'\mathbf{K}_i}\left.\frac{1}{\omega(\mathbf{K}_i)-\omega(-\mathbf{K}_0')-i\gamma_0}\right\rangle\ .\end{aligned} \tag{16d}$$

Here two points are discussed. First the polariton amplitude decays with a decay rate γ_0 through surface transmission and/or inelastic scatterings, e.g., by phonons. This effect is taken into account by replacing e^{-iHt} and e^{iHt} in Eq. (16a) by $e^{-i(H-i\gamma_0)t}$ and $e^{i(H+i\gamma_0)t}$, respectively, and $\omega(\mathbf{K}_0)$ and $\omega(\mathbf{K}_i)$ by $\omega(\mathbf{K}_0)+i\gamma_0$ and $\omega(\mathbf{K}_i)-i\gamma_0$, respectively. Integration in t in Eq. (16c) gives a factor $(2\gamma_0)^{-1}$ in Eq. (16d) taking into account the fact that $\omega_0=\omega(\mathbf{K}_0)$ and $\omega_i=\omega(\mathbf{K}_i)$. This comes from the fact that our system of polaritons is a quasistationary state far from the thermal equilibrium and that a polariton once scattered inelastically cannot contribute again to generation of phase-conjugated wave. This is in contrast to the Anderson localization in metals in thermal equilibrium. Second, we take an ensemble average over a uniform spatial distribution of scattering centers, so that an ensemble average of products of V matrix elements is divided into products of the ensemble average of a pair of V's. Here note that

$$\begin{aligned}\langle V_{\mathbf{q}\mathbf{q}'}V_{\mathbf{k}\mathbf{k}'}\rangle &= \left\langle \sum_i e^{i(\mathbf{q}-\mathbf{q}')\cdot\mathbf{R}_i} V(\mathbf{q}-\mathbf{q}') \sum_j e^{i(\mathbf{k}-\mathbf{k}')\cdot\mathbf{R}_j} V(\mathbf{k}-\mathbf{k}') \right\rangle \\ &= n_i |V(\mathbf{q}-\mathbf{q}')|^2 \delta_{\mathbf{q}-\mathbf{q}',\mathbf{k}'-\mathbf{k}} \\ &\doteqdot n_i |V(0)|^2 \delta_{\mathbf{q}-\mathbf{q}',\mathbf{k}'-\mathbf{k}} \ . \end{aligned} \tag{17}$$

It is also easily understood from these facts that an ensemble average of odd-number products of V's vanishes. First the ensemble averages of scatterings within the leftward propagation of a polariton (on the upper lines in all the diagrams of Fig. 1) and within the rightward one [on the lower lines of the diagrams of Figs. 1(c) and 1(d)] in the density matrix are described, respectively, by the retarded and advanced Green's functions:

$$G^R(\omega_0,\mathbf{q}) = \frac{1}{\omega(\mathbf{K}_0)-\omega(\mathbf{q})+i(\gamma_0+\gamma)} \ ,$$

$$G^A(\omega_i,\mathbf{q}') = \frac{1}{\omega(\mathbf{K}_i)-\omega(\mathbf{q}')-i(\gamma_0+\gamma)} \ .$$

Diagrams of Figs. 2(b) and 2(c) are shown to have singularly dominating contributions to the vertex part Ξ. Only the terms with $n=m$ in Eq. (16d) remain finite for the diagrams of Figs. 2(b) and 2(c) after the ensemble average with respects to impurity sites. Note that the self-energy described by Fig. 2(a) is taken into account in each propagator in the diagrams of Figs. 2(b) and 2(c). Then the vertex part $\Xi(\omega_0-\omega_i)$ is written in terms of contributions from the ladder diagram Γ_l [Fig. 2(b)] and the maximally crossed diagram Γ_c [Fig. 2(c)] as

$$\Xi(\omega_0-\omega_i) = \frac{-i}{2\gamma_0} \frac{1}{\omega(\mathbf{K}_0)-\omega(\mathbf{K}_s)+i(\gamma_0+\gamma)} (\Gamma_l+\Gamma_c) \times \frac{1}{\omega(\mathbf{K}_i)-\omega(-\mathbf{K}_0')-i(\gamma_0+\gamma)} \ . \tag{18}$$

The ladderlike contribution of Fig. 2(b), which is characteristic of a diffusive motion of polariton, is summed up as

$$\Gamma_l = \frac{U_0}{1-U_0X} \ , \tag{19}$$

where $U_0 \equiv n_i|V(0)|^2$ and

$$\begin{aligned} X &= \sum_{\mathbf{q}} G^R(\omega_0,\mathbf{q}) G^A(\omega_i,\mathbf{K}_i-\mathbf{K}_0+\mathbf{q}) \\ &= N(\omega_0) \int d\omega_{\mathbf{q}} \int_0 \frac{\sin\Theta}{2} d\Theta \frac{1}{\omega(\mathbf{K}_0)-\omega(\mathbf{q})+i(\gamma_0+\gamma)} \frac{1}{\omega(\mathbf{K}_i)-\omega(\mathbf{q}+\mathbf{K}_i-\mathbf{K}_0)-i(\gamma_0+\gamma)} \\ &= 2\pi i N(\omega_0) \int \frac{\sin\Theta}{2} d\Theta \frac{1}{\omega_0-\omega_i-(\mathbf{K}_i-\mathbf{K}_0)\cdot\mathbf{v}_g+2i(\gamma_0+\gamma)} \ . \end{aligned} \tag{20}$$

Here summation over $\mathbf{q}$ was replaced by an integral in energy with a state density $N(\omega_0)$. We introduced the group velocity of the polariton at the energy $\omega_{\mathbf{q}}=\omega_0$ as

$$\mathbf{v}_g = \nabla_{\mathbf{q}}\omega_{\mathbf{q}}|_{\omega_{\mathbf{q}}=\omega_0} \ ,$$

and Θ is an angle between a group velocity $\mathbf{v}_g$ and $\mathbf{K}_i-\mathbf{K}_0$. We are interested in the degenerate or nearly degenerate cases so that

$$2(\gamma_0+\gamma) \gg |\omega_0-\omega_i| \quad \text{and} \quad |\mathbf{K}_i-\mathbf{K}_0|v_g \ .$$

Therefore, the energy denominator in Eq. (20) is expanded as follows:

$$\begin{aligned} X &= \frac{\pi N(\omega_0)}{\gamma_0+\gamma} \int_{-1}^{1} \frac{dz}{2} \left[1 - \frac{\omega_0-\omega_i}{2i(\gamma_0+\gamma)} + \frac{|\mathbf{K}_i-\mathbf{K}_0|v_g z}{2i(\gamma_0+\gamma)} - \frac{|\mathbf{K}_i-\mathbf{K}_0|^2 v_g^2 z^2}{8(\gamma_0+\gamma)^2} + \cdots \right] \\ &\doteqdot \frac{\pi N(\omega_0)}{\gamma_0+\gamma} \left[1 + \frac{i(\omega_0-\omega_i)}{2(\gamma_0+\gamma)} - \frac{|\mathbf{K}_i-\mathbf{K}_0|^2 v_g^2}{12(\gamma_0+\gamma)^2} \right] . \end{aligned}$$

Inserting this result into Eq. (19),

$$\Gamma_l(\mathbf{K}_i-\mathbf{K}_0) \doteqdot \frac{2(\gamma_0+\gamma)U_0}{2\gamma_0-i(\omega_0-\omega_i)+D|\mathbf{K}_i-\mathbf{K}_0|^2} \ . \tag{21}$$

Here we used the fact $\gamma \gg \gamma_0$ and a diffusion constant

$$D \equiv \frac{v_g^2}{6(\gamma_0+\gamma)} .$$

Next we evaluate a contribution Γ_c from the series of maximally crossed diagrams of Fig. 2(c). This is done very similarly to the case of Γ_l and is expressed as

$$\Gamma_c = \frac{U_0^2 Y}{1-U_0 Y} ,$$

where $Y=\sum_{\mathbf{q}} G^R(\omega_0,\mathbf{q})G^A(\omega_0',\mathbf{K}_0-\mathbf{K}_0'-\mathbf{q})$. Then we have

$$\Gamma_c(\mathbf{K}_0-\mathbf{K}_0') \doteq \frac{2(\gamma_0+\gamma)U_0}{2\gamma_0 - i(\omega_0-\omega_0')+D|\mathbf{K}_0-\mathbf{K}_0'|^2} .$$

Here we used the fact $U_0 Y \doteq 1$ as $2(\gamma_0+\gamma) \gg |\omega_0-\omega_0'|$ and $D|\mathbf{K}_0-\mathbf{K}_0'|^2$ and denoted the backward pump polariton as $(\omega_0', -\mathbf{K}_0')$. As a result we can conclude that the strongest singularity comes from the maximally crossed diagram for small $2\gamma_0$ under the usual case ($\omega_0=\omega_0'$, $\mathbf{K}_0'=\mathbf{K}_0$) while the ladder contribution is finite as $\mathbf{K}_0 \neq \mathbf{K}_i$ for the generation of the phase-conjugated wave. However, this can also contribute singularly to the backscattering of polariton for a case such as the forward and probe fields being coincident with each other, i.e., $\mathbf{K}_0=\mathbf{K}_i$ and $\omega_0=\omega_i$, and a signal polariton propagates in the direction $\mathbf{K}_s=-\mathbf{K}_i$.

V. GRATING FORMATION WITHOUT SINGULARITIES

In this section, we will discuss the formation of the population grating and generation of a phase-conjugated wave due to the processes described by the diagrams of Figs. 1(a) and 1(b). Then it will be shown that those processes have no singularities obtained in Sec. IV for the processes of Figs. 1(c) and 1(d), but that these bring about a conventional phase-conjugation amplitude without any of the singular enhancements discussed in the last section.

We evaluate first the signal amplitude $\langle c_{\mathbf{K}_s}(\omega_s)\rangle$ for the diagrams of Fig. 1(a) with a combination of input lights given by case IIIa of Table I, i.e., $\omega_1=(\omega_0,\mathbf{K}_0)$, $\omega_2=(\omega_0,-\mathbf{K}_0)$, and $\omega_3=(\omega_i,\mathbf{K}_i)$. It is obtained by procedures similar to those in Sec. III as

$$\begin{aligned}\langle c_{\mathbf{K}_s}(\omega_s)\rangle_a &= (-i)^3 \int_{-\infty}^{\infty} dt\, e^{i\omega_s t} \int_{-\infty}^{t} dt_3 \int_{-\infty}^{t_3} dt_2 \int_{-\infty}^{t_2} dt_1 \langle\langle c_{\mathbf{K}_s} H'(\mathbf{K}_i,t_3)H'(-\mathbf{K}_0,t_2)H'(\mathbf{K}_0,t_1)\rho_0\rangle\rangle \\ &= A \int_{-\infty}^{\infty} dt\, e^{i(\omega_s-2\omega_0+\omega_i)t} \int_0^{\infty} G_s(\tau_3)d\tau_3 \int_0^{\infty} \Xi'(\tau_2)d\tau_2 \int_0^{\infty} G_f(\tau_1)d\tau_1 . \end{aligned} \tag{22}$$

Here A is the same as Eq. (9a), $G_s(\tau_3)$ and $G_f(\tau_1)$ are given by Eqs. (11a) and (11c), respectively, but

$$\Xi'(\tau) = -ie^{2i\omega_0\tau}\langle\langle \omega_s\mathbf{K}_s|e^{-iH\tau}|\omega_0\mathbf{K}_0\rangle_+ \langle \omega_i\mathbf{K}_i|e^{-iH\tau}|\omega_0-\mathbf{K}_0\rangle_+\rangle . \tag{23a}$$

This vertex part describes formation of the population grating and generation of phase-conjugated polariton due to the processes of Figs. 1(a) and 1(b). This is also expanded in the interaction V between polariton and scatterers using Eq. (12a). Here also H is replaced by $H-i_{\gamma_0}$ to take account of the effect from inelastic scatterings and leakage of the polariton to outside the crystal. A product of the first-order expansions in the two propagators in Eq. (23a) shown by the diagram of Fig. 3(a) gives the following result:

$$\int_0^{\infty} \Xi'(\tau_2)d\tau_2 = \frac{-in_i|V(0)|^2}{2\gamma_0} \frac{1}{\omega(\mathbf{K}_0)-\omega(\mathbf{K}_s)+i(\gamma_0+\gamma)} \frac{1}{\omega(-\mathbf{K}_0)-\omega(\mathbf{K}_i)+i(\gamma_0+\gamma)} . \tag{23b}$$

Here the higher-order scatterings within each propagator were taken into account according to the diagram of Fig. 2(a) as already introduced in Sec. III. Next we will show that the higher-order ladder [Fig. 3(b)] and mostly crossed diagrams [Fig. 3(c)] give negligible contribution to the generation of the phase-conjugated wave. The second-order and higher-order ladder and maximally crossed diagrams contain the following integrals:

$$\begin{aligned} X' &= \sum_{\mathbf{k}} \frac{1}{\omega(\mathbf{K}_0)-\omega(\mathbf{k})+i(\gamma_0+\gamma)} \frac{1}{\omega(-\mathbf{K}_0)-\omega(-\mathbf{k})+i(\gamma_0+\gamma)} \\ &\doteq N(\omega_0)\int d\omega \frac{1}{\omega(\mathbf{K}_0)-\omega+i(\gamma_0+\gamma)} \frac{1}{\omega(-\mathbf{K}_0)-\omega+i(\gamma_0+\gamma)} , \end{aligned}$$

and

$$\begin{aligned} Y' &= \sum_{\mathbf{k}} \frac{1}{\omega(\mathbf{K}_0)-\omega(\mathbf{k})+i(\gamma_0+\gamma)} \frac{1}{\omega(-\mathbf{K}_0)-\omega(\mathbf{k}+\mathbf{K}_i-\mathbf{K}_0)+i(\gamma_0+\gamma)} \\ &\doteq N(\omega_0)\int d\omega \frac{1}{\omega(\mathbf{K}_0)-\omega+i(\gamma_0+\gamma)} \frac{1}{\omega(-\mathbf{K}_0)-\omega-(\mathbf{K}_i-\mathbf{K}_0)\cdot\mathbf{v}_g+i(\gamma_0+\gamma)} . \end{aligned}$$

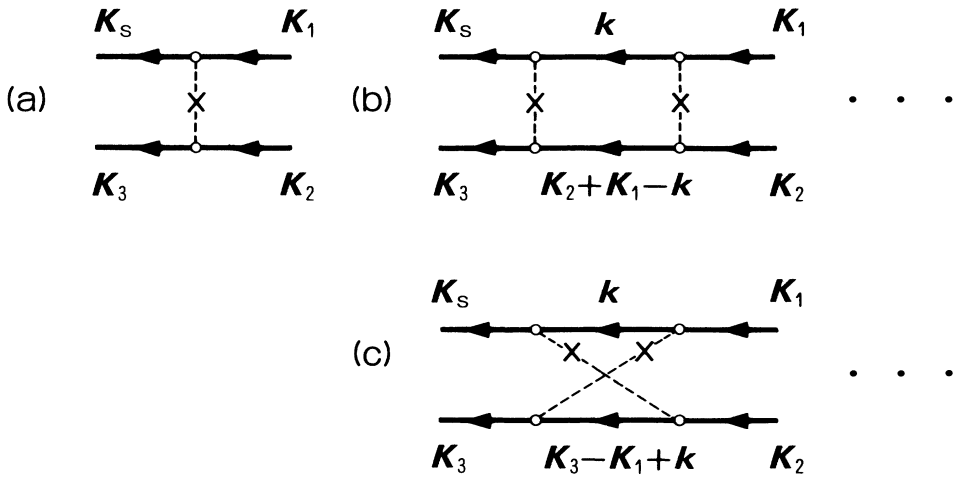

FIG. 3. (a) The lowest-order scattering mechanism of two polaritons which are leftward propagating in the density matrix. (b) Ladderlike scatterings of these two polaritons. (c) Maximally crossed scatterings of these two polaritons by impurities.

These integrals vanish as long as the state density of polariton is approximated as a constant $N(\omega_0)$. This will be justified if ω_0 is far from the polariton bottleneck, and will be discussed in Sec. VII. The polaritons obey Bose statistics so that the Green's function is

$$D(\omega,\mathbf{K})=\frac{1}{\omega^2-\omega_{\mathbf{K}}^2\pm i\delta} .$$

However, it was simplified into the form of Eqs. (13a) and (13b) under the rotating-wave approximation, neglecting a contribution from $-1/(\omega+\omega_{\mathbf{K}}\pm i\delta)$. Taking off this approximation, we have a small contribution of the order of (γ/ω_0) from Figs. 3(b) and 3(c) to the vertex part. However, we may neglect these contributions safely in comparison to those discussed in Secs. III and IV. Therefore, contributions from higher-order scatterings of Figs. 3(b) and 3(c) are negligible. The contribution of Fig. 1(b) is obtained by replacing $G_f(\tau_1)$ in Eq. (22) with $G_b(\tau_1)$. Contributions from the cases of IIIa and IIIb in Table I with $\mathbf{K}_0$ and $-\mathbf{K}_0$ exchanged are also obtained by exchanging $\mathbf{K}_0$ and $-\mathbf{K}_0$ in the above results. This gives the same value beside the factor A of Eq. (19) as long as $\omega(-\mathbf{K}_0)=\omega(\mathbf{K}_0)$.

VI. GENERATION OF A PHASE-CONJUGATED WAVE

The amplitude of the signal wave $(\omega_s,\mathbf{K}_s)$ through the phase-conjugation process is obtained by summing up all contributions of Fig. 1, which were derived in the preceding two sections. The sum of contributions from cases Ic and Id in Table I are also shown as follows:

$$\begin{aligned}\langle c_{\mathbf{K}_s}(\omega_s)\rangle_{c+d}=&2\pi A\delta(\omega_s-2\omega_0+\omega_i)\delta_{\mathbf{K}_0-\mathbf{K}_s,\mathbf{K}_i+\mathbf{K}_0'}\frac{1}{\omega_s-\omega(\mathbf{K}_s)+i(\gamma_0+\gamma)}\\&\times\left[\frac{1}{\omega_0-\omega(\mathbf{K}_0)+i(\gamma_0+\gamma)}-\frac{1}{\omega_0-\omega(-\mathbf{K}_0)-i(\gamma_0+\gamma)}\right]\\&\times\left[\frac{-i}{2\gamma_0}\right](\Gamma_l+\Gamma_c)\frac{1}{\omega(\mathbf{K}_0)-\omega(\mathbf{K}_s)+i(\gamma_0+\gamma)}\frac{1}{\omega(\mathbf{K}_i)-\omega(-\mathbf{K}_0')-i(\gamma_0+\gamma)} ,\end{aligned} \tag{24}$$

where

$$\Gamma_l=\frac{2(\gamma_0+\gamma)U_0}{2\gamma_0-i(\omega_0-\omega_i)+D(\mathbf{K}_i-\mathbf{K}_0)^2} , \tag{24a}$$

$$\Gamma_c=\frac{2(\gamma_0+\gamma)U_0}{2\gamma_0-i(\omega_0-\omega_0')+D(\mathbf{K}_0-\mathbf{K}_0')^2} . \tag{24b}$$

Taking account of Dirac's and Kronecker's delta functions describing conservation laws of energy and wave-number vectors, the last two propagators in Eq. (24), combined with $(2\gamma_0)^{-1}$ and some factors of A and Γ_l and Γ_c, describe the formation of the population grating due to $\mathbf{K}_i$ and $-\mathbf{K}_0'$ polaritons as

$$N_p=\frac{(\boldsymbol{\mu}\cdot\mathbf{E}_{\mathbf{K}_i}^*)(\boldsymbol{\mu}\cdot\mathbf{E}_{-\mathbf{K}_0'})}{2\gamma_0}\times\frac{2(\gamma_0+\gamma)}{[\omega(\mathbf{K}_i)-\omega(-\mathbf{K}_0')]^2+(\gamma_0+\gamma)^2} .$$

On the other hand, the remaining factors of Γ_l and Γ_c, i.e.,

$$\frac{U_0}{2\gamma_0 - i(\omega_0-\omega_i)+D(\mathbf{K}_i-\mathbf{K}_0)^2}$$

and

$$\frac{U_0}{2\gamma_0 - i(\omega_0-\omega_0')+D(\mathbf{K}_0-\mathbf{K}_0')^2} = \frac{U_0}{2\gamma_0 - i(2\omega_0-\omega_i-\omega_s)+D(\mathbf{K}_s+\mathbf{K}_i)^2} ,$$

describe the reflection of polaritons $\mathbf{K}_0$ into the direction $\mathbf{K}_s$ due to the population grating. The factor $2\gamma_0$ in the denominators in Eqs. (24a) and (24b) means a cutoff frequency within which the reflection works effectively. The other contribution to the generation of the phase-conjugated wave comes from Figs. 1(a) and 1(b) with combinations of input waves IIIa and IIIb in Table I. These are summed up into the same form as Eq. (24) but a sum of Γ_l and Γ_c is replaced by U_0. Therefore, these give the conventional expression for generation of a phase-conjugated wave. This contribution is smaller by a factor of $(\gamma_0+\gamma)/\gamma_0$ than those of Ic and Id in Table I.

We will discuss the relative importance among these contributions to the phase conjugation of the polariton. For usual experimental conditions, the diagram of Figs. 1(c) and 1(d) with a combination of input polaritons Ic and Id in Table I has the dominating contribution to the generation of the phase-conjugated wave. Usually a phase-conjugated wave is induced by the degenerate four-wave mixing of $(\omega_0,\mathbf{K}_0)$, $(\omega_0,-\mathbf{K}_0)$, and $(\omega_i=\omega_0,\mathbf{K}_i)$. Therefore, the energy denominator of Eq. (24b) becomes $2\gamma_0$ for the mostly crossed diagram of Figs. 1(c) and 1(d). Contribution from the ladderlike diagram for the process of Figs. 1(c) and 1(d) has a finite denominator as $\mathbf{K}_i \neq \mathbf{K}_0$ for observation of the phase-conjugated wave as shown by Eq. (24a). A value of $D(\mathbf{K}_i-\mathbf{K}_0)^2$ is usually much larger than $2\gamma_0$, e.g., for exciton polaritons in CuCl. The vertex part of Figs. 1(a) and 1(b) has U_0 instead of Γ_l and Γ_s. Therefore, these contributions to $\langle c_{\mathbf{K}_s}(\omega_0)\rangle$ are smaller by a factor of $\gamma_0/(\gamma_0+\gamma)\ll 1$ than those of Figs. 1(c) and 1(d), as already mentioned. Therefore, we may conclude that the diagrams of Figs. 1(c) and 1(d) with the combinations of input polariton Ic and Id in Table I have the dominant contribution to generation of the phase-conjugated wave. The expression of Eq. (24) is simplified by taking account of the fact that $\omega_0=\omega(\mathbf{K}_0)=\omega(-\mathbf{K}_0)$, $\omega_s=\omega(\mathbf{K}_s)$, and $\omega_s=\omega_i=\omega_0$, or $|\omega_0-\omega_s|,|\omega_0-\omega_i|\ll 2\gamma$,

$$\langle c_{\mathbf{K}_s}(\omega_s)\rangle \doteq 2\pi A\,\delta(\omega_s-2\omega_0+\omega_i) \times \frac{1}{\gamma_0(\gamma_0+\gamma)^3}\,\frac{2U_0}{2\gamma_0 - i(\omega_0-\omega_0')+D(\mathbf{K}_0-\mathbf{K}_0')^2} . \tag{25}$$

This comes from the maximally crossed diagrams given by Fig. 2(c) through the four-wave mixing shown in Figs. 1(c) and 1(d). Note that the maximally crossed diagram represents a coherent superposition of forward- and backward-propagating polaritons, reflecting a time-reversal invariance of the system.

VII. DISCUSSION AND CONCLUSION

Effects of the weak localization were clearly demonstrated in the dc resistance of thin disordered metallic films and metal-oxide-semiconductor (MOS) inversion layers as a function of temperature.[19–21] These linear responses could pick up the singularity at $\omega=0$ and $\mathbf{q}=0$ of the time-reversal collective modes ("cooperons").[13] The linear optical response, however, is insensitive to these collective modes even though the exciton polaritons suffer from weak localization. On the other hand, the weak localization of polaritons has been shown in this paper to play a key role in nonlinear optical responses, especially in generation of the phase-conjugated wave. This is because we can control the difference of the two input frequencies, $\omega_0-\omega_i$, and a combination of the two wave vectors near the singular point of the collective excitations, i.e., $\omega_0-\omega_i=0$ and $\mathbf{q}=\mathbf{K}_0-\mathbf{K}_0'=\mathbf{0}$ as shown in Sec. III. Generation of the phase-conjugated wave, which is time-reversal propagation of the probe light, has been shown to actually originate from the singularity due to coherent superposition of the forward- and backward-propagating waves of polaritons under elastic multiple scatterings at impurities, reflecting the time-reversal symmetry of the system.

We will list some characteristics of the phase-conjugated wave generated by the present mechanism. Observation of these characteristics will also serve to check the present theory. The phase-conjugated wave is generated dominantly by the maximally crossed diagram of Fig. 1(c). Here the vertex part Γ_c in Eq. (24b) describes the microscopic process of phase conjugation. Therefore, let us study first the characteristics of Γ_c. The phase conjugation was observed already near the exciton-frequency region of CuCl (Ref. 22) and the polaritons of this material have been studied very well,[23] so we will especially study the case of CuCl. The group velocity v_g of the polariton ranges from $\hbar K/M\sim 1.2\times 10^6$ cm/sec to $c/(\epsilon_\infty)^{1/2}=1.3\times 10^{10}$ cm/sec. As far as the incident frequency is limited below the upper polariton and above the polariton bottleneck, the group velocity changes from 0.2×10^6 to 3.0×10^6 cm/sec.[24] The value of $\hbar(\gamma_0+\gamma)$ depends also on the incident frequency as well as the samples, e.g., the concentration of impurities. This is observed as the spectrum half-width at half maximum of the intensity of the hyper-Raman scattering leaving the polariton in the final state.[25] It ranges from $\hbar(\gamma_0+\gamma)=0.05$ to 2.0 meV. The inelastic scattering rate γ_0 was observed as a function of temperature and γ_0 may almost be determined by the polariton transmission through surfaces and nonradiative decay below 40 K. The lifetime $\tau_0=(2\gamma_0)^{-1}$ is tentatively set to be of the order of a nanosecond, i.e., $\hbar\gamma_0\sim 0.03$ meV.[26] Therefore, $D\equiv v_g^2/6(\gamma_0+\gamma)$ is estimated to be of the order of 1 cm^2/sec so that $D(\mathbf{K}_0-\mathbf{K}_0')^2$ is much larger than $2\gamma_0$ as long as the deviation of the angle between $\mathbf{K}_0$ and $-\mathbf{K}_0'$ from π is larger than 2.2×10^{-2} rad.

(1) The first characteristic of the present theory is the singular dependence of $\langle c_{\mathbf{K}_s}(\omega_s)\rangle$ through Γ_c on $\omega_0-\omega_0'$ and $\mathbf{K}_0-\mathbf{K}_0'$. For the degenerate four-wave mixing $\omega_0=\omega_i=\omega_s$, the intensity $|\langle c_{\mathbf{K}_s}(\omega_s)\rangle|^2$ of the phase-conjugated wave is very sensitive to an angle $(\pi-\theta)$ between the two pump fields $\mathbf{K}_0$ and $-\mathbf{K}_0'$. As far as $\theta>2.2\times10^{-2}$ rad, the signal intensity is proportional to $(1-\cos\theta)^{-2}\doteqdot 4\theta^{-4}$.

(2) On the other hand, when we use nongenerate four-wave mixing, we will be able to determine the dispersion of the collective mode from the dependence

$$|\langle c_{\mathbf{K}_s}(\omega_s)\rangle|^2 \propto \{(\omega_0-\omega_0')^2+[2\gamma_0+D(\mathbf{K}_0-\mathbf{K}_0')^2]^2\}^{-1} . \tag{26}$$

(3) The diffusion constant $D\equiv v_g^2/6(\gamma_0+\gamma)$ can be varied by changing the input frequency ω_0 over several orders of magnitude as the group velocity v_g depends sensitively on the input frequency over the polariton dispersion. This brings about the incident frequency dependence of the phase-conjugated wave intensity even for the degenerate case with the fixed θ.

(4) The cutoff frequency $2\gamma_0$ in Eq. (26) is sensitive to the lattice temperature $T>40$ K.

(5) The signal depends also on the polarizations of three input fields as shown in Table I. This comes from the expression A in Eq. (9a). These dependences were already observed by Mizutani and Nagasawa.[22]

As to the characteristics (3), the approximation of a constant density of states will become poor around the bottleneck on the polariton dispersion. Elaborate calculation is also being done taking into account the change of the density of states to clarify the mobility edge as a function of impurity concentration.[27] Phase conjugation associated with two-photon excitation of an excitonic molecule has already been observed.[22] The signal amplitude due to this process is calculated by the diagrams of Figs. 1(a) and 1(b) taking account of the exciton-exciton attractive interaction. This is skipped here as it is not directly related to the Anderson localization of polaritons. As the vertex part Γ_c shows, the formation of polariton gratings and reflection of one pump wave into the conjugated wave are enhanced in proportion to the square of impurity concentration n_i through $2(\gamma_0+\gamma)U_0$. However, the intensity of the phase-conjugated wave depends reversely on the impurity concentration n_i for the case of $\gamma\gg\gamma_0$ as follows:

$$\langle c_{\mathbf{K}_s}(\omega_s)\rangle \sim n_i^{-2} \quad \text{for } D(\mathbf{K}_0-\mathbf{K}_0')^2\ll 2\gamma_0 \tag{27a}$$

$$\sim n_i^{-1} \quad \text{for } D(\mathbf{K}_0-\mathbf{K}_0')^2\gg 2\gamma_0 . \tag{27b}$$

This is because the propagation of the input as well as the signal polaritons is incoherently scattered by impurities, although the grating formation as well as the reflection due to the grating are enhanced by the impurity scatterings through Γ_c. Note that we cannot extrapolate the results of Eq. (27) to the limit $n_i\to 0$ as these are restricted to the case $\gamma\equiv\pi N(\omega_0)n_i|V(0)|^2\gg\gamma_0$. Of course, $\langle c_{\mathbf{K}_s}(\omega_s)\rangle$ vanishes in the limit of $n_i|V(0)|^2\equiv U_0\to 0$, as Eq. (25) shows.

The present theory has clarified microscopic mechanisms of the phase-conjugation processes, in which the weak localization of polaritons plays important roles. It is also capable of clarifying the problem of polariton dynamics as observed by Kuwata and Nagasawa.[28] They observed the generation of backward-propagating polaritons under pumping by the forward wave, and the strong coupling among the forward and backward polaritons. This can also be understood[27] by the weak localization of polaritons presented in this paper.

ACKNOWLEDGMENTS

The author thanks Dr. N. Nagaosa and N. Taniguchi for fruitful discussions. This work was partially supported by Grant-in-Aid No. 63604516 for Scientific Research on Priority Area, New Functionality Materials—Design, Preparation, and Control—by the Ministry of Education, Science, and Culture of Japan.

[1]E. Abrahams, P. W. Anderson, D. C. Licciardello, and T. V. Ramakrishnan, Phys. Rev. Lett. **42**, 673 (1979).

[2]For general review on Anderson localization see, G. Bergmann, Phys. Rev. **107**, 1 (1984); P. A. Lee and T. V. Ramakrishnan, Rev. Mod. Phys. **57**, 287 (1985); *Anderson Localization,* edited by Y. Nagaoka [Prog. Theor. Phys. Suppl. **84**, (1985)]; *Anderson Localization,* edited by Y. Nagaoka and H. Fukuyama (Springer-Verlag, Berlin, 1982).

[3]D. A. de Wolf, IEEE Trans. Antennas Propag. **19**, 254 (1971); Y. Kuga, L. Tsang, and A. Ishimaru, J. Opt. Soc. Am. A **2**, 616 (1985).

[4]M. P. Van Albada and Ad Lagendijk, Phys. Rev. Lett. **55**, 2692 (1985).

[5]P. E. Wolf and G. Maret, Phys. Rev. Lett. **55**, 2696 (1985).

[6]E. Akkermans, P. E. Wolf, and R. Maynard, Phys. Rev. Lett. **56**, 1471 (1986).

[7]S. Etemad, R. Thompson, and M. J. Andrejco, Phys. Rev. Lett. **57**, 575 (1986).

[8]M. Kaveh, M. Rosenbluh, I. Edrei, and I. Freund, Phys. Rev. Lett. **57**, 2049 (1986).

[9]M. P. Van Albada, M. B. van der Mark, and Ad Lagendijk, Phys. Rev. Lett. **58**, 361 (1987).

[10]E. Akkermans and R. Maynard, Phys. Rev. B **32**, 7850 (1985).

[11]J. L. Langer and T. Neal, Phys. Rev. Lett. **16**, 984 (1966); D. Vollhardt and D. Wölfle, Phys. Rev. B **22**, 4666 (1980).

[12]For general review on optical phase conjugation, A. Yariv, IEEE J. Quantum Electron. **QE-14**, 650 (1978); C. Giuliano, Physics Today **34** (7), 27 (1981); Y. R. Shen, *The Principles of Nonlinear Optics* (Wiley, New York, 1984), Chap. 14.

[13]H. Fukuyama, J. Phys. Soc. Jpn. **50**, 3407 (1981); Prog. Theor. Phys. Suppl. **84**, 47 (1985).

[14]J. J. Hopfield, Phys. Rev. **112**, 1555 (1958).

[15]S. Mukamel and E. Hanamura, Phys. Rev. A **33**, 1099 (1986).

[16]E. Hanamura, in *Advances in Multi-photon Processes and Spec-*

troscopy, edited by S. H. Lin (World Scientific, Singapore, 1987), Vol. 3, p. 1.
[17]E. Hanamura, Phys. Rev. B **37**, 1273 (1988).
[18]E. Hanamura, Phys. Rev. B **38**, 1228 (1988).
[19]G. J. Dolan and D. D. Osheroff, Phys. Rev. Lett. **43**, 721 (1979).
[20]S. Kobayashi, F. Komori, Y. Ootuka, and W. Sasaki, J. Phys. Soc. Jpn. **49**, 1635 (1980).
[21]L. Van den dries, C. Van Haesendonck, Y. Bruynseraede, and G. Deutscher, Phys. Rev. Lett. **46**, 565 (1981).
[22]G. Mizutani and N. Nagasawa, J. Phys. Soc. Jpn. **52**, 2251 (1983).
[23]M. Ueta, H. Kanzaki, K. Kobayashi, Y. Toyozawa, and E. Hanamura, *Excitonic Processes in Solids* (Springer-Verlag, Berlin, 1986), Chaps. 2 and 3.
[24]Y. Masumoto, Y. Unuma, Y. Tanaka, and S. Shionoya, J. Phys. Soc. Jpn. **47**, 1844 (1979).
[25]T. Itoh, T. Katohno, T. Kirihara, and M. Ueta, J. Phys. Soc. Jpn. **53**, 854 (1984).
[26]M. Kuwata, J. Phys. Soc. Jpn. **53**, 4456 (1984).
[27]N. Taniguchi and E. Hanamura (unpublished).
[28]M. Kuwata and N. Nagasawa, Solid State Commun. **45**, 937 (1983).